Spectrochimica Acta Part A: Molecular and Biomolecular Spectroscopy 254 (2021) 119620

Contents lists available at ScienceDirect

Spectrochimica Acta Part A: Molecular and Biomolecular Spectroscopy

journal homepage: www.elsevier.com/locate/saa

A highly sensitive and selective fluorescence turn-on probe for the sensing of H_2S *in vitro* and *in vivo*

Qi Sun [a,1], Heng Liu [c,1], Yuan Qiu [a], Jun Chen [a], Feng-Shou Wu [a], Xiao-Gang Luo [a,d], Da-Wei Wang [b,*]

[a] *Key Laboratory for Green Chemical Process of Ministry of Education and School of Chemistry and School of Chemistry and Environmental Engineering, Wuhan Institute of Technology, Wuhan 430205, China*
[b] *State Key Laboratory of Elemento-Organic Chemistry, and Department of Chemical Biology, National Pesticide Engineering Research Center, Collaborative Innovation Center of Chemical Science and Engineering, College of Chemistry, Nankai University, Tianjin 300071, China*
[c] *Institute of Functional Materials and Molecular Imaging, Key Laboratory of Emergency and Trauma, Ministry of Education, Key Laboratory of Hainan Trauma and Disaster Rescue, College of Clinical Medicine, College of Emergency and Trauma, Hainan Medical University, Haikou 571199, China*
[d] *School of Materials Science and Engineering, Zhengzhou University, No.100 Science Avenue, Zhengzhou City 450001, Henan Province, China*

HIGHLIGHTS

- A novel fluorescent probe **NT-SH** was constructed for sensing of H_2S.
- The probe **NT-SH** exhibited high sensitivity to detect H_2S in aqueous solution.
- The probe **NT-SH** could be used for imaging of H_2S in living A549 cells and zebrafish model.

GRAPHICAL ABSTRACT

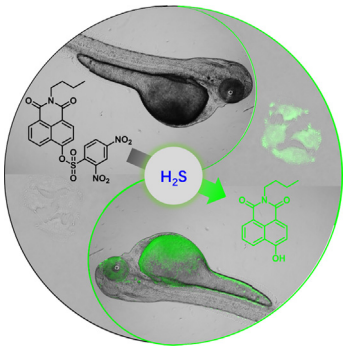

ARTICLE INFO

Article history:
Received 28 August 2020
Received in revised form 22 January 2021
Accepted 9 February 2021
Available online 26 February 2021

Keywords:
Fluorescent probe
Hydrogen sulfide
Bioimaging
Zebrafish

ABSTRACT

A fluorescence turn-on probe, 2-butyl-1,3-dioxo-2,3-dihydro-1H-benzo[de]isoquinolin-6-yl 2,4-dinitrobenzenesulfonate (**NT-SH**), has been constructed for sensing of hydrogen sulfide (H_2S). **NT-SH** exhibited excellent detection performance including favorable water solubility, low fluorescence background, high enhancement (45-fold), large linear response range (0–50 μM) and low detection limit (80.01 nM) for H_2S in aqueous. In addition, the response mechanism of **NT-SH** for H_2S was confirmed by the theoretical calculation and mass spectral analysis. More importantly, the imaging experiments of H_2S *in vitro* and *in vivo* confirmed that **NT-SH** had low cytotoxicity, and favorable biocompatibility. In addition, it illustrated that **NT-SH** was able to detected exogenous H_2S in living cells and zebrafish. These results suggested that **NT-SH** can be act as a potential molecular tool for detecting of H_2S in aqueous solution, *in vitro* and *in vivo*.

1. Introduction

Hydrogen sulfide (H_2S) is a toxic gas with the smell of rotten eggs. It is a vital endogenous gas molecule, similar to CO and NO [1–5]. The H_2S is able to be produced by three different enzyme catalyzed processes including cystathionine γ-lyase (CSE),

* Corresponding author.
E-mail address: wangdw@nankai.edu.cn (D.-W. Wang).
[1] These authors contributed equally to this work.

https://doi.org/10.1016/j.saa.2021.119620
1386-1425/

cystathionine β-synthase (CBS) and 3-mercaptopyruvate sulfurtransferase (3-MST)/cysteine aminotransferase (CAT) in various tissues and organs [6–9]. In addition, H_2S is closely related to various physiological pathways, such as inflammation, apoptosis, vasodilation, angiogenesis, neuromodulation, insulin signaling, oxygen sensing and ischemia reperfusion injury [10–14]. Furthermore, accumulating evidence confirms that the imbalance level of H_2S will lead to a series of diseased such as liver cirrhosis, Down syndrome, Alzheimer's disease, diabetes, cirrhosis and heart disease [15–18]. Nevertheless, these possible molecular events of H_2S and its specific mechanisms are still unclear. Therefore, in order to investigate H_2S biology and H_2S-related diseases, efficient technology and method for visualization of H_2S in cells and animal model is an imperative solving problem.

Fluorescence probe detection technology are the most powerful method for the detection of H_2S in complicated biological systems owing to its simple, rapid response, good sensitivity, high sensitivity and non-invasive [19–21]. To date, a great quantity of fluorescent probes have been constructed and applied to the detection of intracellular H_2S [22,23]. These fluorescent probes for H_2S are designed based on three mechanisms including reduction of azides and nitro/azanol to amines, nucleophilic reaction of Michael addition and formation of copper sulfide precipitation [24–30]. Although many great successes of fluorescent probes for H_2S have been reported, only few of them are used for real-time imaging and sensing of H_2S *in vivo* (Table S1).

Herein, we rationally constructed a fluorescent turn-on probe **NT-SH** for sensitive and selective sensing of H_2S *in vitro* and *in vivo*. The construction of **NT-SH** contained two parts: the naphthalimide part was acted as the fluorophore and the 2,4-dinitrobenzenesulfonyl (DNBS) part was acted as the quenching group via photoinduced electron transfer (PET) effect and recognition group for reaction with H_2S, as illustrated in Scheme 1. **NT-SH** exhibited excellent water solubility, low fluorescence background and good biocompatibility due to the obvious advantages of naphthalimide fluorophore. More importantly, **NT-SH** was applied for sensing and visualizing of H_2S in A549 cells and zebrafish with low fluorescence background and high sensitivity, which revealed **NT-SH** had the potential ability for imaging and detection of H_2S *in vitro* and *in vivo*.

2. Materials and methods

2.1. Materials and instruments

All the reagents used in the experiments were analytical grade reagents obtained from Sigma-Aldrich. These reagents could be directly used without further purification. The A549 living cells and zebrafish larvae were purchased from China Zebrafish Resource Center (Wuhan city of China). The PBS buffers with different pH were prepared by STARTER 3100C pH meter. The ^1H and ^{13}C NMR spectrums were tested using a Varian Inova 500 NMR Spectrometer. The UV–vis and fluorescence spectra were recorded by multifunctional enzyme labeling instrument (SpectraMax M5, USA). The fluorescence images of A549 cells and zebrafishes were performed by inverted fluorescence microscopy (Olympus IX71, Japan).

General Optical Measurements. 10 mM **NT-SH** was dissolved in DMOS as the stock solution. The PBS buffers with different pH (4.0, 5.0, 6.0, 7.0, 7.4, 8.0 and 9.0) were prepared for testing the pH effect. Various analytes (100 μM) including inorganic metal salt ($FeSO_4$, $HgCl_2$, CuCl, $BaCl_2$, $MnSO_4$, $NaNO_3$, NaF, NaI, NaCl, CH_3-COONa), and amino acids (Leu, Cys, Asp, Arg) were prepared to evaluate selectivity. All the test concentrations of **NT-SH** used in the spectra experiment and bioimaging were 10 μM, which were diluted from the stock solution. The excitation wavelength of all fluorescence spectra was 450 nm.

Limit of detection. The limit of detection (LOD) was calculated depending on the following formula (1), which was reported in the previous literatures [31–33]. The fluorescence spectrums of probe **NT-SH** were measured for 10 times to obtain the standard deviation σ. The linear relationship between the fluorescence intensity (550 nm) and the dose of NaHS was measured to get the slop k.

$$\mathrm{LOD} = 3\sigma/\mathrm{k} \tag{1}$$

Quantum yield. The fluorescence quantum yields of **NT-SH** and **NT** were detected according to following Eq. (2) based on the reported literatures [34–36]. The subscripts c and s represented fluorescein (Φ = 0.98) and sample respectively. Φ was the quantum yield of the reference compound and samples. The subscripts A represented the absorbance and the subscripts F mean the fluorescence integral area.

$$\Phi_s = \frac{F_s \cdot A_c}{F_c \cdot A_s}\Phi_c \tag{2}$$

Cell Imaging. A549 cells were cultured in RPMI-1640 complete medium including penicillin and streptomycin on a cell culture flask in the cell incubator. A549 cells were initial digested by trypsin, and then cultured overnight on a 12-well plate. After incubation with **NT-SH** (10 μM) for 30 min, the A549 cells were washed three times to remove the remaining **NT-SH**. Then, various doses of NaHS (0, 25, 50 and 100 μM) were adding into the A549 cells for next 30 min. Finally, the A549 cells was imaged at green channel (510–550 nm) by the Olympus IX71 microscope.

Zebrafish Imaging. zebrafish was cultured in 100 mL medium containing 1-phenyl-2-thiourea (PTU) at 28 °C for 48 h. For the imaging experiments, 10 μM **NT-SH** was adding into the cultured medium of zebrafishes at 28 °C for 1 h. Then, the medium containing **NT-SH** was carefully removed to reduce the fluorescence background. And the zebrafish was imaged directly as the control group. In the experimental groups, these zebrafishes were further co-cultured with various doses of NaSH (0, 25, 50, 100 μM) for 2 h. Finally, all the zebrafishes were imaged at green channel (510–550 nm) by Olympus SZX16 microscope.

3. Results and discussion

3.1. Design and synthesis of probe NT-SH

As we know, naphthalimide was a widely used fluorophore due to its practical advantages, such as large Stokes' shift, high quantum yield, favorable water solubility and biocompatibility [37,38]. Base on this, a water-soluble fluorescence probe **NT-SH** for sensing of H_2S was constructed by connecting the recognition group DNBS and the fluorophore **NT** via a simple nucleophilic reaction, as shown in Scheme 1. **NT-SH** probe showed a low fluorescence background due to the PET effect of DNBS group. while the breaking sulfonate bond by H_2S produced fluorescence turn-on phenomenon through the released of fluorophore. To evaluate the response performance of **NT-SH** for H_2S, **NT-SH** and **NT** were synthesized according to the synthetic route, as displayed in Scheme S1. These synthesized compounds were identified by ^1H NMR, ^{13}C NMR and HR-MS in the Support Information, as shown in Figs. S1-S9.

Spectra response of NT-SH toward H_2S. As shown in Fig. S10, the pK_{a1} and pK_{a2} of hydrogen sulfide are calculated to be 6.88 and 14.15, respectively. Therefore, under the test condition (pH = 7.4), the main forms of H_2S are HS^- and S^{2-} *in vitro* and *in vivo*. Hence, NaHS can be used as a source of H_2S. To verify the response capa-

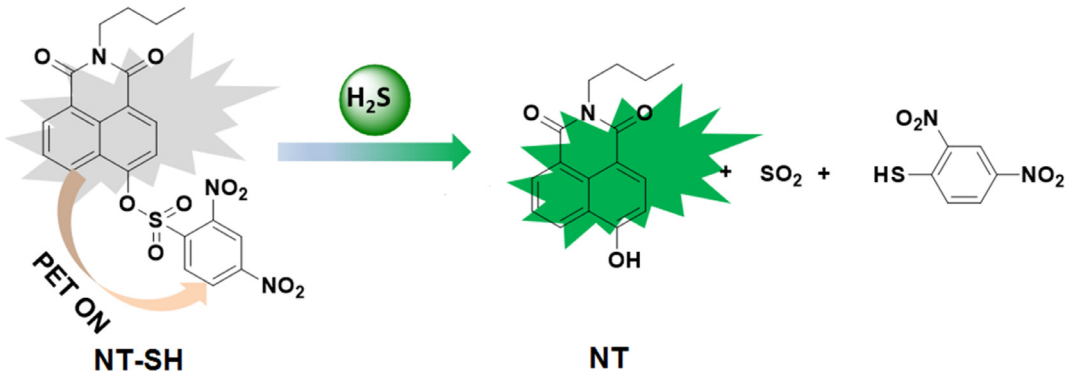

Scheme 1. Sensing Mechanism of Fluorescent Probe **NT-SH** for H_2S.

bility of **NT-SH**, the UV–vis absorption spectra and fluorescence spectra were measured for sensing of H_2S in PBS buffer (10 mM, pH 7.4). As depicted in Fig. 1a, the free probe **NT-SH** exhibited obvious absorption peak at 355 nm. After adding NaSH to the solution, the peak was red shift to 450 nm. In the fluorescence spectra, as shown in Fig. 1b, the probe **NT-SH** showed almost no fluorescence (Φ = 0.003), which illustrated that **NT-SH** had extremely low background. After treatment with NaSH, the peak at 560 nm sharp increased (Φ = 0.046) compared to free probe **NT-SH.** These results confirmed that probe **NT-SH** had a good response to H_2S. In order to detail analyze the sensitivity of **NT-SH** to H_2S, the time-dependent and dose-dependent experiments were investigated. As illustrated in Fig. 1c, the emission spectra of **NT-SH** with NaHS gave a significant fluorescence turn-on response. Moreover, this time-course fluorescence intensity at 560 nm was gradually enhanced in 30 min. After reaction with NaHS, the fluorescence enhancement was calculated to be 45 folds. These optical data indicated that probe **NT-SH** was able to specifically sense H_2S by the fluorescence turn-on signal. To further inspect the detection limit of **NT-SH** towards H_2S, the fluorescence spectra of **NT-SH** with different doses of H_2S (0–500 μM) was studied, as shown in Fig. 1d. Obviously, the fluorescence intensity at 560 nm was remarkable enhanced with the increased doses of NaHS (0–300 μM) and reached maximum value in the range of 300–500 μM, as depicted

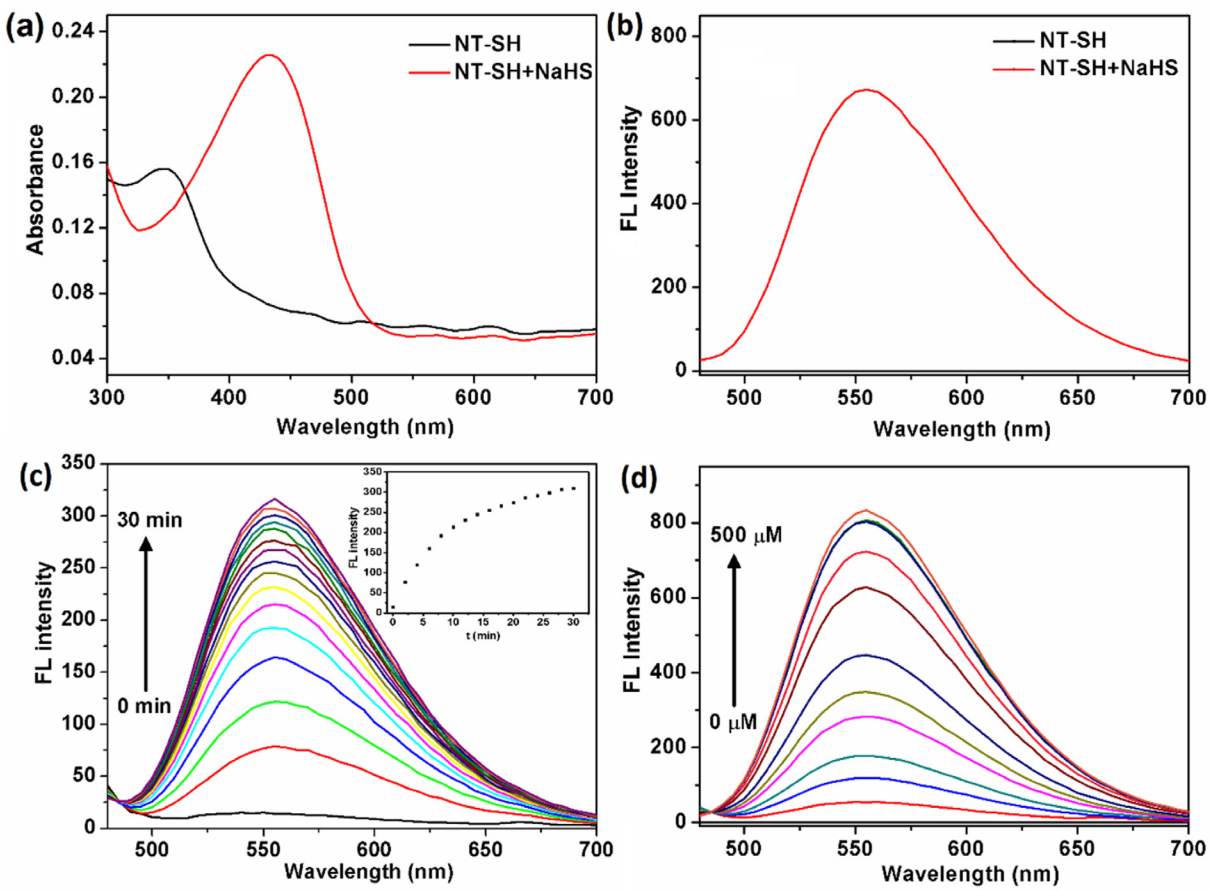

Fig. 1. UV–vis absorption spectrum (a) and fluorescence spectrum (b) of **NT-SH** (10 μM) with or without NaSH. (c) Fluorescence spectrum of **NT-SH** (10 μM) incubated with NaHS for different time (0–30 min). (d) Fluorescence spectra of **NT-SH** (10 μM) co-incubated with various doses of NaHS (0–500 μM) for 30 min. The test condition was PBS buffer, λ_{ex} = 450 nm.

in Fig. S11. In particular, the fluorescence intensity at 560 nm was linear with the dose of H_2S (0–50 μM) (R^2 = 0.995) (Fig. S12). Therefore, the LOD of **NT-SH** for H_2S was calculated to be ~ 80.01 nM. These results explained that probe **NT-SH** could determine H_2S with high efficiency and sensitivity.

Sensing Mechanism. To investigate the sensing mechanism of **NT-SH** for sensing of H_2S, we analyzed the reaction solution of **NT-SH** and H_2S using HRMS assay. As shown in Fig. S13, after the reaction solution was incubated at room temperature for 30 min, a compound with m/z = 269.1030 was detected, corresponding to the fluorophore **NT** $[M + H]^+$ (calculated for 269.1052). Therefore, based on the results of HRMS analysis, we proposed that the mechanism of the synthesized probe **NT-SH** in sensing of H_2S was that H_2S acted as a nucleophilic attack reagent to attack the **NT-SH**, and cleavaged the bond between naphthalimide ring and 2,4-dinitrobenzene group, which in turn releasing the fluorophore **NT** (Scheme1).

Theoretical Calculations. To confirm the quench mechanism of probe **NT-SH**, we performed the density functional theory (DFT) calculation studies of **NT-SH** and **NT** with Gaussian 09 software at B3LYP/6-31G(d) level [39,40]. As illustrated in Fig. 2, the 2,4-dinitrobenzene group and the naphthalimide ring of the probe **NT-SH** almost lie in two different planes, and the two different planes was nearly in parallel, which led to fluorescence quenching. Additionally, both HOMO and LOMO π-electrons of fluorophore **NT** were all located around the naphthalimide ring. While, the HOMO π-electrons of **NT-SH** were all locate around its naphthalimide ring, and the LUMO π-electrons of **NT-SH** were all locate on. The distribution of the HOMO and LUMO π-electrons of **NT-SH** indicated that, **NT-SH** was possibly quenched by the PET process. In the **NT-SH**, the electrons transferred from naphthalimide ring (PET donor) to the 2,4-dinitrobenzene group (PET acceptor), which in turn significantly reduced the fluorescence of naphthalimide moiety. This process is corresponding to the fluorescence "turn-off" we have observed in the experiments. Upon reacting with H_2S, the PET effect of **NT-SH** was destroyed and released the fluorophore **NT**, which made the fluorescence "turn-on".

Selectivity of NT-SH. The selectivity was investigated to evaluated the sensing ability of **NT-SH.** Several analytes included thiols (Cys and H_2S), cations (Fe^{2+}, Hg^{2+}, Cu^+, Ba^{2+}, Mn^{2+}), anions (NO_2^-, Br^-, SO_3^{2-}, F^-, I^-, Cl^-, CH_3COO^-) and amino acids (Leu, Asp, Arg) were incubated with **NT-SH** for 30 min and the fluorescent signals at 560 nm were tested accordingly. As shown in Fig. 3, compared with Cys, the response of **NT-SH** to H_2S was two times higher than that of Cys, which was reported as a common interfering agent of thiol probe [41,42]. Furthermore, the fluorescence enhancement data revealed that **NT-SH** showed no response to the other species, including cations, anions and non-thiol amino acids. It confirmed that **NT-SH** exhibited relative high selectivity for H_2S compared with anions, cations and thiol-free amino acids.

pH effect. The effect of pH of **NT-SH** toward H_2S was determined for studied its potential biological applications. As shown in Fig. S14, the fluorescence signal of **NT-SH** with and without H_2S was measured in the pH range of 4.0–10.0. In absence of H_2S, negligible fluorescence changes of free **NT-SH** were observed, suggesting **NT-SH** had an excellent stability in an extensive pH range. Moreover, when reaction with H_2S, the fluorescence signal of **NT-SH** increased sharply over the pH range (4.0–7.4) and reduce gradually at the pH value of 7.4–10.0. Notably, it verified that the optimal pH value of **NT-SH** for detection of H_2S was 7.4. These results indicated that **NT-SH** was able to detect H_2S under physiological conditions.

Living Cell Imaging. To evaluate the imaging performance of **NT-SH** for H_2S *in vitro*, the human lung cancer cell line (A549) was selected as the imaging model. First, the cytotoxicity of **NT-SH** at various doses (0, 1, 5, 10, 20 and 30 μM) against A549 was studied. As shown in Fig. S15, the results indicated that **NT-SH** was suitable for the cell imaging due to extremely low cytotoxicity. Based on this, the cell imaging of **NT-SH** for 100 μM NaHS at different incubation times (0, 30, 60 and 90 min) was tested, as depicted in Fig. S16. The experiment results illustrate that the green fluorescence signal exhibited gradually enhance and reached the maximum value at 60 min. Meanwhile, the imaging performance of **NT-SH** for various doses of NaHS was further studied. As depicted

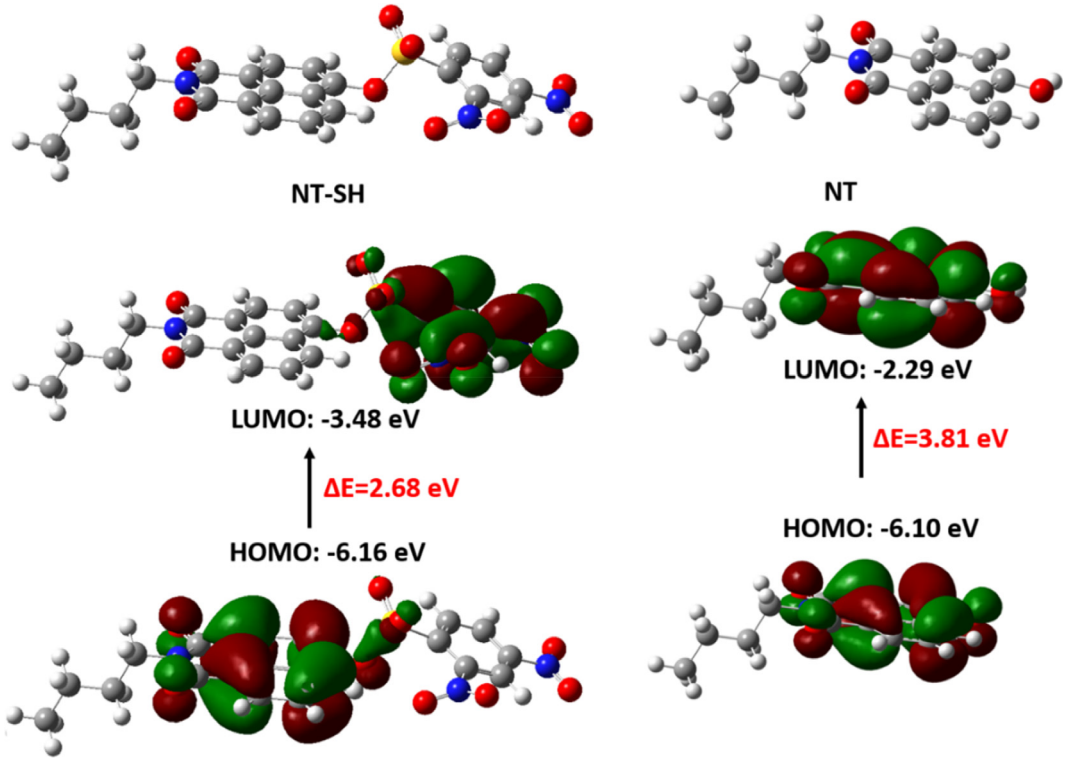

Fig. 2. Theoretical studies of **NT** and **NT-SH**. The HOMO and LUMO values of **NT-SH** and **NT** were calculated by Gaussian 09 at B3LYP/6-31G(d) level.

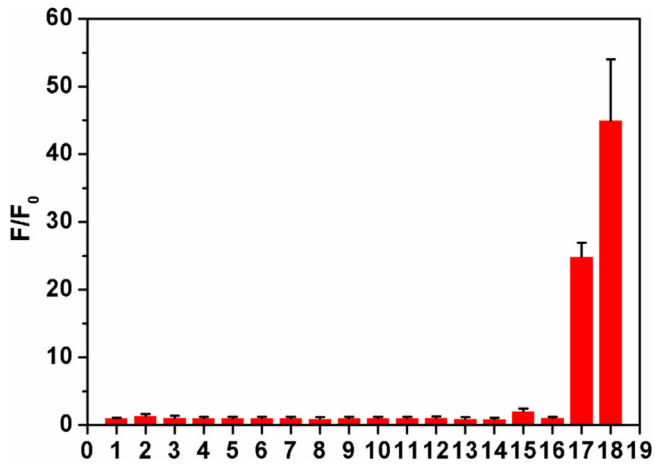

Fig. 3. (a) Fluorescence response of **NT-SH** (10 μM) aganist different interfering analytes. (1. Blank, 2. Fe^{2+}, 3. Hg^{2+}, 4. Cu^{2+}, 5. Ba^{2+}, 6. Mn^{2+}, 7. NO_3^-, 8. Br^-, 9.SO_3^{2-}, 10. F^-, 11. I^-, 12. Cl^- 13. CH_3COO^-, 14. Leu, 15. Asp, 16. Arg, 17. Cys, 18. NaHS) The concentration of analytes was 100 μM.

in Fig. 4, no fluorescence was noticed when A549 cells were only pretreated with **NT-SH** for 30 min, (Fig. 4a, e, i). Conversely, after incubation with NaHS (10, 50 and 100 μM) for 30 min, the fluorescence signal was enhanced with the increase doses of NaHS (Fig. 4-f-h). These results could be confirmed via the optical data which was calculated from the corresponding green fluorescence photograph (Fig. 4m). These results suggested that **NT-SH** could be utilized as a sensitive probe for monitoring and imaging exogenous H_2S in living cells.

Zebrafish Imaging. Zebrafish, a kind of classical model organism, was widely used for fluorescence imaging [43–45]. Thus, the imaging performance of **NT-SH** for H_2S against zebrafish was further studied due to its perfect imaging effect in living cells, as depicted in Fig. 5. Zebrafishes were initial preincubated with **NT-SH** (10 μM) for 1 h to make sure that **NT-SH** could be penetrated into zebrafish. These zebrafishes were washed with incubation medium to remove the remaining **NT-SH** and then treated with various doses of NaHS (10, 50 and 100 μM) for 2 h. All the zebrafishes were imaging at the green channel. As expected, the zebrafish was still alive without NaHS, and apparently without fluorescence, indicating

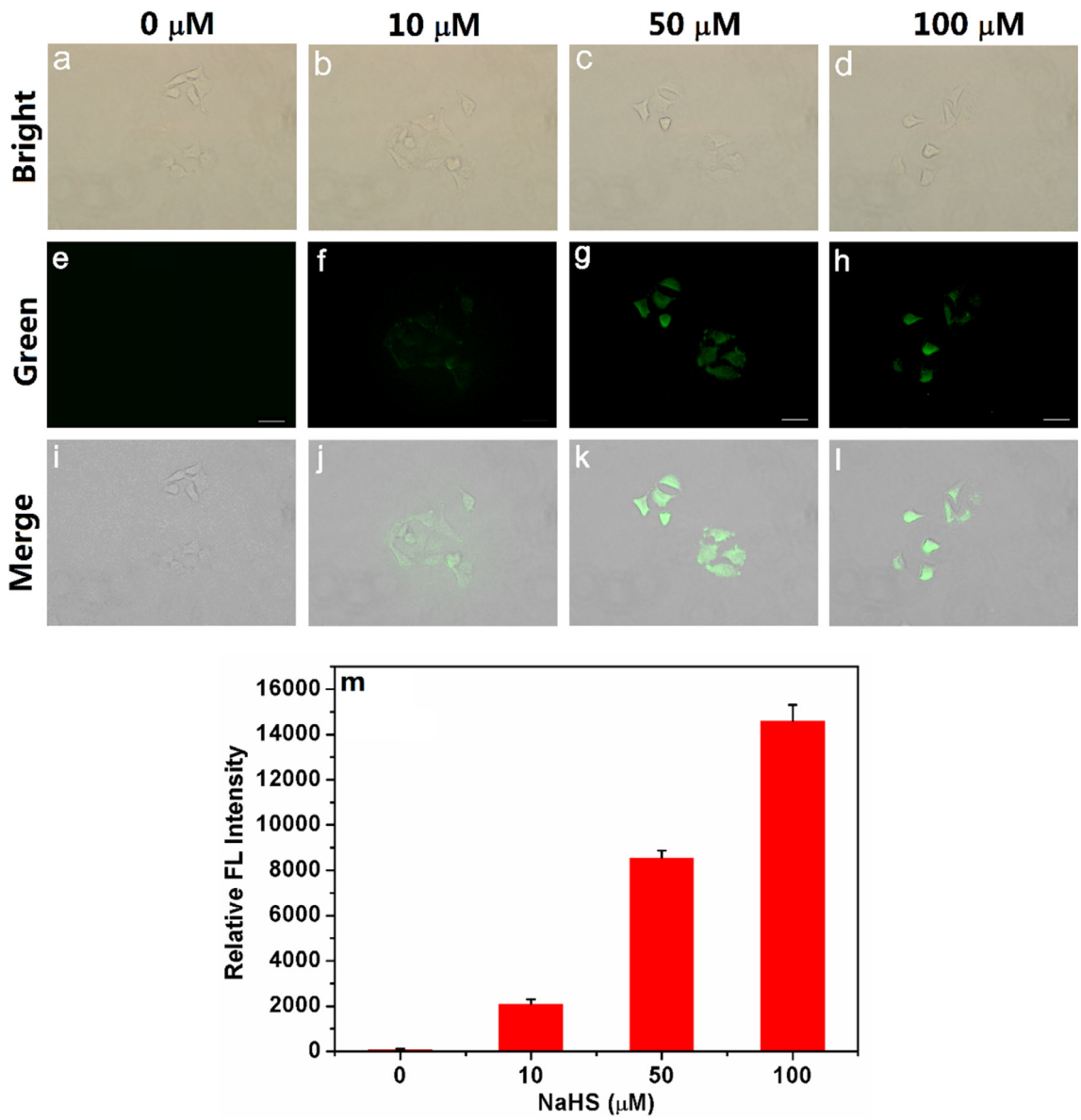

Fig. 4. Cell imaging of **NT-SH** with different concentrations of NaHS (0, 10, 50 and 100 μM) for 30 min. (m) Relative fluorescence intensity of A549 cells at the green channel (e, f, g and h). Data represent mean standard error (n = 3), scale bar = 40 μm.

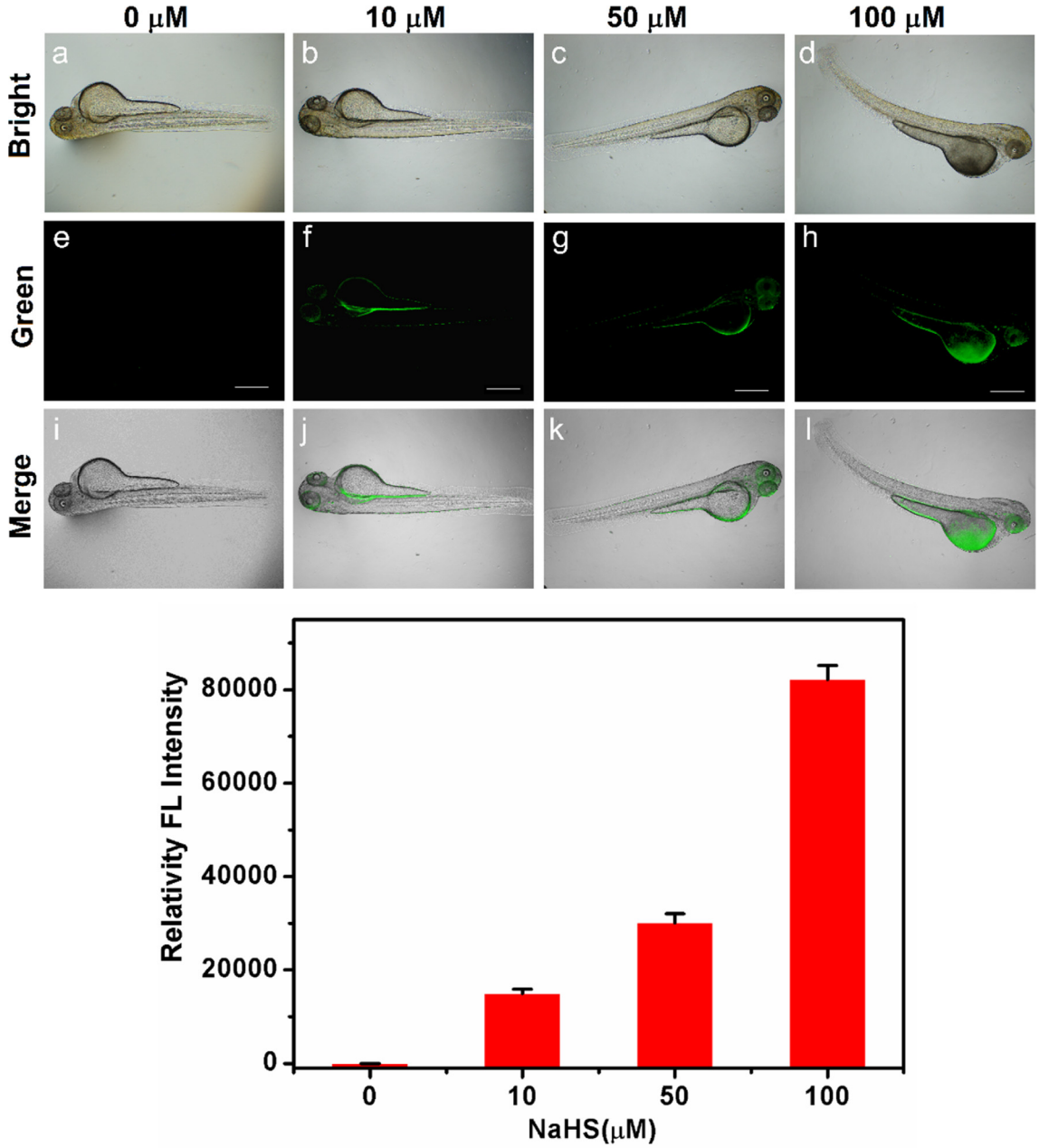

Fig. 5. Zebrafishes imaging of **NT-SH** (10 μM) with various doses of NaHS (0, 10, 50 and 100 μM). (m) Relative fluorescence intensity of zebrafish in the green channel (e, f, g and h). Data represent mean standard error (n = 3), scale bar = 200 μm.

that **NT-SH** had low toxicity and fluorescence background for imaging in zebrafish (Fig. 5a, e, i). In addition, in the presence of NaHS, the fluorescence signal of the zebrafishes was clearly noticed and obviously enhanced with the increase doses of NaHS (Fig. 5f-h). The relative fluorescence intensity of the fluorescence photograph illustrated that **NT-SH** could detect and image exogenous H_2S (Fig. 5m). All the results revealed that **NT-SH** could be applied for imaging of H_2S in zebrafish with high sensitivity.

4. Conclusion

In summary, we have constructed a new turn-on fluorescent probe **NT-SH** for the sensing of H_2S in water solution, living cells and zebrafish. **NT-SH** was a water soluble, low fluorescence background and cytotoxicity probe which exhibited high selectivity, fluorescence enhancement (45-fold), large linear response range (0–50 μM) and low limit of detection (80.01 nM). In addition, the possible sensing mechanism of **NT-SH** for H_2S was proven via theory calculation and mass spectral analyses, which confirmed a PET process based on cleavage DNS group. Furthermore, the fluorescence imaging of **NT-SH** treated with NaHS revealed that **NT-SH** was able to apply for the detection of exogenous H_2S in living cells and zebrafish model due to its excellent biocompatibility. Therefore, this new probe **NT-SH** had a potential to be serve as an efficient tool for sensing of H_2S *in vitro* and *in vivo*.

CRediT authorship contribution statement

Qi Sun: Methodology, Data curation, Writing - original draft. **Heng Liu:** Methodology, Data curation. **Yuan Qiu:** Methodology, Writing - original draft. **Jun Chen:** Formal analysis, Data curation. **Feng-Shou Wu:** Investigation. **Xiao-Gang Luo:** Investigation, Software. **Da-Wei Wang:** Supervision, Project administration, Funding acquisition.

Declaration of Competing Interest

The authors declare that they have no known competing financial interests or personal relationships that could have appeared to influence the work reported in this paper.

Acknowledgment

This work was financially supported by the National Natural Science Foundation of China (21804102), the National Key R&D Program of China (2017YFE0118200), Special Projects of the Central Government in Guidance of Local Science and Technology Development in Hubei Province (2020ZYYD040), the second batch of the Key Research and Development Project of Hubei Province (2020BAB073), the Outstanding Young and Middle-aged Scientific Innovation Team of Colleges and Universities of Hubei Province (T201908).

Appendix A. Supplementary data

Supplementary data to this article can be found online at https://doi.org/10.1016/j.saa.2021.119620.

References

[1] D. Gong, X. Zhu, Y. Tian, S.C. Han, M. Deng, A. Iqbal, W. Liu, W. Qin, H. Guo, A phenylselenium-substituted BODIPY fluorescent turn-off probe for fluorescence imaging of hydrogen sulfide in living cells, Anal. Chem. 89 (2017) 1801–1807.
[2] H. Wang, D. Yang, R. Tan, J.Z. Zhang, R. Xu, F.Z. Zhang, Y. Zhou Jun, A cyanine-based colorimetric and fluorescence probe for detection of hydrogen sulfide in vivo, Sens. Actuators B Chem. 247 (2017) 883–888.
[3] R. Wang, Physiological implications of hydrogen sulfide: a whiff exploration that blossomed, Physiol. Rev. 92 (2012) 791–896.
[4] G.K. Kolluru, X. Shen, S.C. Bir, C.G. Kevil, Hydrogen sulfide chemical biology: pathophysiological roles and detection, Nitric Oxide 35 (2013) 5–20.
[5] X. Zhang, W. Qu, H. Liu, Y. Ma, L. Wang, Q. Sun, F. Yu, Visualizing hydrogen sulfide in living cells and zebrafish using a red-emitting fluorescent probe via selenium-sulfur exchange reaction, Anal. Chim. Acta 1109 (2020) 37–43.
[6] M.D. Hammers, M.J. Taormina, M.M. Cerda, L.A. Montoya, D.T. Seidenkranz, R. Parthasarathy, M.D. Pluth, A bright fluorescent probe for H_2S enables analyte-responsive, 3D imaging in live zebrafish using light sheet fluorescence microscopy, J. Am. Chem. Soc. 137 (2015) 10216–10223.
[7] L. Wei, Z. Zhu, Y. Li, L. Yi, Z. Xi, A highly selective and fast-response fluorescent probe for visualization of enzymatic H_2S production in vitro and in living cells, Chem. Commun. 51 (2015) 10463–10466.
[8] H. Kimura, Hydrogen sulfide: its production, release and functions, Amino Acids 41 (2011) 113–121.
[9] N. Shibuya, S. Koike, M. Tanaka, M. Ishigami Yuasa, Y. Kimura, Y. Ogasawara, K. Fukui, N. Nagahara, H. Kimura, A novel pathway for the production of hydrogen sulfide from D-cysteine in mammalian cells, Nat. Commun. 4 (2013) 1366–1369.
[10] W. Yang, E.J. Sacks, M.L.L. Ivey, S.A. Miller, D.M. Francis, Resistance in lycopersicon esculentum intraspecific crosses to race T1 strains of xanthomonas campestris pv. vesicatoria causing bacterial spot of tomato, Phytopathology 95 (2005) 519–527.
[11] K. Eto, T. Asada, K. Arima, T. Makifuchi, H. Kimura, Brain hydrogen sulfide is severely decreased in alzheimer's disease, Biochem. Bioph. Res. Co. 293 (2002) 1485–1488.
[12] S. Fiorucci, E. Antonelli, A. Mencarelli, S. Orlandi, B. Renga, G. Rizzo, E. Distrutti, V. Shah, A. Morelli, The third gas: H_2S regulates perfusion pressure in both the isolated and perfused normal rat liver and in cirrhosis, Hepatology 42 (2005) 539–548.
[13] K. Módis, Y. Ju, A. Ahmad, A.A. Untereiner, Z. Altaany, L. Wu, C. Szabó, R. Wang, S-sulfhydration of ATP synthase by hydrogen sulfide stimulates mitochondrial bioenergetics, Pharmacol. Res. 113 (2016) 116–124.
[14] Y.H. Liu, M. Lu, L.F. Hu, T.H. Wong, G.D. Webb, J.S. Bian, Hydrogen sulfide in the mammalian cardiovascular system, Antioxid. Redox Sign. 17 (2012) 141–185.
[15] B.D. Paul, S.H. Snyder, H_2S signalling through protein sulfhydration and beyond, Nat. Rev. Mol. Cell Biol. 13 (2012) 499–507.
[16] B.D. Paul, S.H. Snyder, Gasotransmitter hydrogen sulfide signaling in neuronal health and disease, Biochem. Pharmacol. 149 (2018) 101–109.
[17] H.J. Wei, X. Li, X.Q. Tang, Therapeutic benefits of H_2S in alzheimer's disease, J. Clin. Neurosci. 21 (2014) 1665–1669.
[18] P. Kamoun, M.C. Belardinelli, A. Chabli, K. Lallouchi, B. Chadefaux-Vekemans, Endogenous hydrogen sulfide overproduction in down syndrome, Am. J. Med. Genet. A. 116A (2003) 310–311.
[19] M.H. Lee, J.S. Kim, J.L. Sessler, Small molecule-based ratiometric fluorescence probes for cations, anions, and biomolecules, Chem. Soc. Rev. 44 (2015) 4185–4419.
[20] M.H. Lee, J.L. Sessler, J.S. Kim, Disulfide-based multifunctional conjugates for targeted theranostic drug delivery, Acc. Chem. Res. 48 (2015) 2935–2946.
[21] M.H. Lee, E.J. Kim, H. Lee, H.M. Kim, M.J. Chang, S.Y. Park, K.S. Hong, J.S. Kim, J.L. Sessler, Liposomal texaphyrin theranostics for metastatic liver cancer, J. Am. Chem. Soc. 138 (2016) 16380–16387.
[22] V.S. Lin, W. Chen, M. Xian, C.J. Chang, Chemical probes for molecular imaging and detection of hydrogen sulfide and reactive sulfur species in biological systems, Chem. Soc. Rev. 44 (2015) 4596–4618.
[23] F. Yu, X. Han, L. Chen, Fluorescent probes for hydrogen sulfide detection and bioimaging, Chem. Commun. 50 (2014) 12234–12249.
[24] S. Wang, S. Xu, G. Hu, X. Bai, T.D. James, L. Wang, A fluorescent chemodosimeter for live-cell monitoring of aqueous sulfides, Anal. Chem. 88 (2015) 1434–1439.
[25] H.A. Henthorn, M.D. Pluth, Mechanistic insights into the H_2S-mediated reduction of aryl azides commonly used in H_2S detection, J. Am. Chem. Soc 137 (2015) 15330–15336.
[26] Y. Qian, J. Karpus, O. Kabil, S.Y. Zhang, H.L. Zhu, R. Banerjee, J. Zhao, C. He, Selective fluorescent probes for live-cell monitoring of sulphide, Nat. Commun. 2 (2011) 495.
[27] H. Li, Q. Yao, J. Fan, N. Jiang, J. Wang, J. Xia, X. Peng, A fluorescent probe for H_2S in vivo with fast response and high sensitivity, Chem. Commun. 51 (2015) 16225–16228.
[28] S. Singha, D. Kim, H. Moon, T. Wang, K.H. Kim, Y.H. Shin, J. Jung, E. Seo, S.J. Lee, K.H. Ahn, Toward a selective, sensitive, fast-responsive, and biocompatible two-photon probe for hydrogen sulfide in live cells, Anal. Chem. 87 (2015) 1188–1195.
[29] Z. Hai, Y. Bao, Q. Miao, X. Yi, G. Liang, Pyridine-biquinoline-metal complexes for sensing pyrophosphate and hydrogen sulfide in aqueous buffer and in cells, Anal. Chem. 87 (2015) 2678–2684.
[30] M. Sun, H. Yu, H. Li, H. Xu, D. Huang, S. Wang, Fluorescence signaling of hydrogen sulfide in broad pH range using a copper complex based on binol-benzimidazole ligands, Inorg. Chem. 54 (2015) 3766–3772.
[31] H. Xu, M. Hepel, "Molecular beacon"-based fluorescent assay for selective detection of glutathione and cysteine, Anal. Chem. 83 (2011) 813–819.
[32] Y. Zhou, J. Yan, N. Zhang, D. Li, S. Xiao, K. Zheng, A ratiometric fluorescent probe for formaldehyde in aqueous solution, serum and air using aza-cope reaction, Sens. Actuators B Chem. 258 (2017) 156–162.
[33] T. Wang, Y. Chai, S. Chen, G. Yang, C. Lu, J. Nie, C. Ma, Z. Chen, Q. Sun, Y. Zhang, J. Ren, F. Wang, W.H. Zhu, Near-infrared fluorescent probe for imaging nitroxyl in living cells and zebrafish model, Dyes Pigm. 166 (2019) 260–265.
[34] J. Li, Y. Cui, C. Bi, S. Feng, F. Yu, E. Yuan, S. Xu, Z. Hu, Q. Sun, D. Wei, J. Yoon, Oligo (ethylene glycol)-functionalized ratiometric fluorescent probe for the detection of hydrazine in vitro and vivo, Anal. Chem. 91 (2019) 7360–7365.
[35] S. Yuan, F. Wang, G. Yang, C. Lu, J. Nie, Z. Chen, J. Ren, Y. Qiu, Q. Sun, C. Zhao, W. H. Zhu, A highly sensitive ratiometric self-assembled micellar nanoprobe for nitroxyl and its application in vivo, Anal. Chem. 90 (2018) 3914–3919.
[36] Z. Zhou, F. Wang, G. Yang, C. Lu, J. Nie, Z. Chen, J. Ren, Q. Sun, C. Zhao, W.H. Zhu, A ratiometric fluorescent probe for monitoring Leucine aminopeptidase in living cells and zebrafish model, Anal. Chem. 89 (2017) 11576–11582.
[37] Z. Xu, J. Yoon, D.R. Spring, A selective and ratiometric Cu^{2+} fluorescent probe based on naphthalimide excimer-monomer switching, Chem. Commun. 46 (2010) 2563–2565.
[38] A.P.D. Silva, H.Q.N. Gunaratne, J.L. Habib-Jiwan, C.P. Mccoy, T.E. Rice, J.P. Soumillion, New fluorescent model compounds for the study of photoinduced electron transfer: the influence of a molecular electric field in the excited state, Angew. Chem. Int. Ed. 34 (1995) 1728–1731.
[39] X. Zhang, Z. Wang, Z. Guo, N. He, P. Liu, D. Xia, X. Yan, Z. Zhang, A novel turn-on fluorescent probe for selective sensing and imaging of glutathione in live cells and organisms, Analyst 144 (2019) 3260–3266.
[40] J. Zhang, X. Bao, J. Zhou, F. Peng, H. Ren, X. Dong, W. Zhao, A mitochondria-targeted turn-on fluorescent probe for the detection of glutathione in living cells, Biosens. Bioelectron. 85 (2016) 164–170.
[41] S. Chen, P. Hou, B. Zhou, X. Song, J. Wu, H. Zhang, J.W. Foley, A red fluorescent probe for thiols based on 3-hydroxyflavone and its application in living cell imaging, RSC Adv. 3 (2013) 11543–11546.
[42] M. Lan, J. Wu, W. Liu, H. Zhang, W. Zhang, X. Zhuang, P. Wang, Highly sensitive fluorescent probe for thiols based on combination of PET and ESIPT mechanisms, Sens. Actuators B Chem. 156 (2011) 332–337.
[43] S. Hu, T. Wang, J. Zou, Z. Zhou, C. Lu, J. Nie, C. Ma, G. Yang, Z. Chen, Y. Zhang, Q. Sun, Q. Fei, J. Ren, F. Wang, Highly chemoselective fluorescent probe for the detection of tyrosinase in living cells and zebrafish model, Sens. Actuators B Chem. 283 (2019) 873–880.
[44] X. Zhang, H. Liu, Y. Ma, W. Qu, H. He, X. Zhang, S. Wang, Q. Sun, F. Yu, Development of a novel near-infrared fluorescence light-up probe with a large stokes shift for sensing of cysteine in aqueous solution, living cells and zebrafish, Dyes Pigm. 171 (2019) 107722.
[45] Q. Sun, Y. Qiu, J. Chen, F.S. Wu, X.G. Luo, Y.R. Guo, X.Y. Han, D.W. Wang, A colorimetric and fluorescence turn-on probe for the detection of palladium in aqueous solution and its application in vitro and in vivo, Spectrochim. Acta. A. 239 (2020) 118547.